THE JOURNAL OF BIOLOGICAL CHEMISTRY VOL. 286, NO. 43, pp. 37849–37857, October 28, 2011

Crystal Structures of Multicopper Oxidase CueO Bound to Copper(I) and Silver(I)

FUNCTIONAL ROLE OF A METHIONINE-RICH SEQUENCE[*S]

Received for publication, August 12, 2011, and in revised form, September 1, 2011 Published, JBC Papers in Press, September 8, 2011, DOI 10.1074/jbc.M111.293589

Satish K. Singh[‡], Sue A. Roberts[‡], Sylvia F. McDevitt[§], Andrzej Weichsel[‡], Guenter F. Wildner[‡], Gregor B. Grass[¶], Christopher Rensing[‖], and William R. Montfort[‡1]

From the Departments of [‡]Chemistry and Biochemistry and [‖]Soil, Water, and Environmental Science, University of Arizona, Tucson, Arizona 85721, the [§]Biology Department, Skidmore College, Saratoga Springs, New York 12866, and the [¶]Bundeswehr Institute of Microbiology, 80937 Munich, Germany

Background: The multicopper oxidase CueO allows *Escherichia coli* to survive in aqueous solutions with a high copper concentration.
Results: Cu(I) and Ag(I) ions coordinate to a flexible, methionine-rich sequence.
Conclusion: The methionine-rich insert and a substrate-binding site ensure that only Cu(I) is oxidized.
Significance: Understanding how bacteria survive in the presence of normally toxic concentrations of metal ions may lead to better antibacterial agents.

The multicopper oxidase CueO oxidizes toxic Cu(I) and is required for copper homeostasis in *Escherichia coli.* Like many proteins involved in copper homeostasis, CueO has a methionine-rich segment that is thought to be critical for copper handling. How such segments function is poorly understood. Here, we report the crystal structure of CueO at 1.1 Å with the 45-residue methionine-rich segment fully resolved, revealing an N-terminal helical segment with methionine residues juxtaposed for Cu(I) ligation and a C-terminal highly mobile segment rich in methionine and histidine residues. We also report structures of CueO with a C500S mutation, which leads to loss of the T1 copper, and CueO with six methionines changed to serine. Soaking C500S CueO crystals with Cu(I), or wild-type CueO crystals with Ag(I), leads to occupancy of three sites, the previously identified substrate-binding site and two new sites along the methionine-rich helix, involving methionines 358, 362, 368, and 376. Mutation of these residues leads to a ~4-fold reduction in k_{cat} for Cu(I) oxidation. Ag(I), which often appears with copper in nature, strongly inhibits CueO oxidase activities *in vitro* and compromises copper tolerance *in vivo*, particularly in the absence of the complementary copper efflux *cus* system. Together, these studies demonstrate a role for the methionine-rich insert of CueO in the binding and oxidation of Cu(I) and highlight the interplay among *cue* and *cus* systems in copper and silver homeostasis.

In *Escherichia coli*, two chromosomally encoded systems, *cue* and *cus*, respond to copper stress by expressing proteins that either oxidize Cu(I) to less toxic Cu(II) or expel excess copper from the cell (1, 2). The *cue* regulon codes for the Cu(I) oxidizing multicopper oxidase CueO, the subject of this report (3, 4), and the Cu(I) translocating P-type ATPase, CopA (5). The expression of both CopA and CueO are up-regulated by CueR, a transcription factor activated by Cu(I) (6, 7). Under anaerobic conditions where CueO is rendered inactive, or when the *cue* system is overwhelmed by high copper concentrations, the *cus* system is activated (1). The *cus* system functions to remove periplasmic Cu(I) (3, 8) and codes for four proteins, a three-component CusCBA copper efflux pump, and the periplasmic copper chaperone CusF (9, 10). Under aerobic conditions, the *cus* system appears redundant for copper homeostasis (1, 11).

Ag(I), a Cu(I) mimic, also induces the *cus* and *cue* systems and the gene products can bind and transport Ag(I) efficiently (5, 11–13). The *cus* system, in fact, was originally identified as a Ag(I) inducible, Ag(I) detoxifying system, rather than a copper detoxifying system (11). Cu(I)-binding sites in proteins can often bind Ag(I), raising the possibility that either ion may compromise the detoxification of the other ion (see for example, Ref. 14). The possibility for combined Cu(I)/Ag(I) stress is common, occurring, for example, in hospitals (15), public health water systems (16), and copper mines, which are often also a source of silver (AgCl or Ag_2S). How bacteria cope with combined Cu(I) and Ag(I) stresses, and how the handling of either ion is influenced by the presence of the other, is not known. The apparent redundancy of the *cus* system in aerobic copper detoxification and its ability to provide moderate Ag(I) detoxification raises the possibility that the *cus* system may function to overcome Ag(I) poisoning of the *cue* system.

* This work was supported, in whole or in part, by National Institutes of Health Grant HL062969 (to W. R. M.) and grants from the International Copper Association (to G. B. G. and C. R.). Portions of this research were carried out at the Stanford Synchrotron Radiation Lightsource, a national user facility operated by Stanford University on behalf of the U.S. Dept. of Energy, Office of Basic Energy Sciences, and at Argonne National Laboratory.
[S] The on-line version of this article (available at http://www.jbc.org) contains supplemental Figs. S1–S4.
The atomic coordinates and structure factors (codes 3OD3, 3NSC, 3NT0, 3NSD, 3NSY, and 3NSF) have been deposited in the Protein Data Bank, Research Collaboratory for Structural Bioinformatics, Rutgers University, New Brunswick, NJ (http://www.rcsb.org/).
[1] To whom correspondence should be addressed: 1041 E. Lowell St., Tucson, AZ 85721. Tel.: 520-621-1884; Fax: 520-626-9204; E-mail: montfort@email.arizona.edu.

CueO is a member of the multicopper oxidase (MCO)[2] family, which includes ascorbate oxidase, laccase, ceruloplasmin, Fet3p, and PcoA (17, 18). All MCOs couple four one-electron substrate oxidation steps to the four-electron reduction of dioxygen to water (19). Cu(I) is the best substrate so far identified for CueO and the likely major substrate for CueO *in vivo* (20, 21). MCOs contain four copper atoms, designated type 1 (T1), type 2 (T2), and two type 3 (T3). The T1 copper gives rise to an absorption peak at 610 nm in UV-visible spectra and the intense blue color typical of MCO proteins. The T2 and two T3 copper atoms form a trinuclear center (TNC) and give rise to a peak in the region of ~330 nm (19). Substrates are oxidized near the T1 copper site, releasing an electron that is shuttled through the T1 site to the TNC, where dioxygen binds and is reduced to water.

The T1 copper in CueO, unlike with laccases (22), is buried in the protein interior (23, 24) (Fig. 1). A 45-residue insert (residues 355–399) containing 14 methionines and five histidines, blocks solvent access to the T1 site and contributes ligands to an additional copper-binding site that must be occupied for full CueO activity (24). Organic compounds and Fe(II) are therefore only substrates for CueO in the presence of excess copper. We originally termed this additional site the regulatory copper site (rCu) for its role in stimulating CueO activity (24), but have renamed it the substrate copper site (sCu) in view of its Cu(I) substrate binding role. Much of the methionine-rich insert has been disordered and unseen in previous CueO structures (23–25). Similar methionine-rich regions are found in other proteins involved in copper homeostasis and are thought to have roles involving copper binding and transport. Prominent examples include the copper importer Ctr1 in *Saccharomyces cerevisiae* (26), PcoA and PcoC, both from the plasmid-based copper resistance system in *E. coli* (17). In Ctr1, a methionine-rich motif occurs at the N terminus and is required for Cu(I) transport across the cytoplasmic membrane, whereas in PcoC, a methionine-rich motif lies at the dimerization interface, suggesting that methionine-rich regions are involved in protein-protein interactions (27). It has also been suggested that PcoC transfers Cu(I) ions bound at its solvent-exposed methionine motifs by docking with the methionine-rich region of the MCO PcoA, which then oxidizes the transferred Cu(I) (21). The MCO CopA from the plasmid encoded *cop* system in *Pseudomonas syringae* binds up to seven additional copper atoms (28). Although these examples provide strong evidence supporting copper binding and transport by methionine-rich motifs, structural characterization of Cu(I) binding at these sites has been lacking.

Here, we have determined the complete structure of the CueO methionine-rich insert and its binding to Cu(I) and Ag(I). We also make use of mutagenic, kinetic, and cell growth experiments to uncover the role for these residues in the handling of both copper and silver.

[2] The abbreviations used are: MCO, multicopper oxidase; T1D, T1 copper depleted (C500S mutant CueO); T1, type 1; T2, type 2; T3, type 3; sCu; substrate copper; TNC, trinuclear center.

EXPERIMENTAL PROCEDURES

Strains, Growth Media, and Copper Tolerance Assay—Wild-type *E. coli* strain W3110 and *cus*-deleted strain W3110 Δ*cusCFBA*::*cat* (GR6) (4) were used for copper tolerance assays using Luria Bertani (LB) media lacking NaCl as the growth media. Strain BL21-DE3 was used for protein expression and grown in regular LB media. Ampicillin (100 μg/ml) was added to growth media as appropriate. For copper tolerance assays, overnight cultures of W3110 or GR6 were diluted 1:500 with fresh LB media (without NaCl) and grown for 2 h at 37 °C, with shaking at 200 rpm. This culture was diluted 1:500 using fresh LB media (without NaCl) in the presence or absence of 5 μM $AgNO_3$ and different concentrations of $CuSO_4$, and grown at 37 °C, with shaking at 200 rpm. After 15 h, the optical density at 600 nm wavelength was measured to monitor growth.

Mutagenesis and Protein Isolation—Three forms of wild-type CueO and two site-specifically mutated CueO proteins were used in this study. Of these, four proteins have been produced recombinantly in fusion with a C-terminal *Strep*-Tag II affinity epitope and isolated from *E. coli* cells, as previously described (3, 20). These are wild-type CueO (tagged) (3), apo-CueO (same as wild-type CueO but without copper cofactor), C500S CueO (containing a Cys^{500} to Ser mutation, leading to loss of the type 1 copper) (24), and ΔMet CueO (containing Met to Ser mutations for methionines 358, 361, 362, 364, 366, and 368). We also produced CueO without any purification tag or extraneous linker sequences, referred to herein as untagged CueO.

C500S CueO was constructed using a PCR-based approach as previously described (20, 24). Untagged CueO and ΔMet CueO were generated from the wild-type CueO insert (EcoRI and PstI) in plasmid pASK-IBA3 (IBA, Göttingen, Germany) as the template in a PCR-based approach using the following primers. The forward and reverse primers for untagged CueO were 5′-AAA TCT AGA TAA CGA GGG CAA AAA ATG CAA CGT GAT TTC TTA AAA TAT TC-3′, and 5′-AAA CTG CAG *TTA* TAC CGT AAA CCC TAA CAT CAT CCC-3′. The forward and reverse primers for ΔMet CueO were 5′-TAT GGA **T**CC GA**G** **T**CT CGA T**TC** G**TC** **C**GG GA**G** **C**CA G**TC** GCT AA**G** **T**GA GAA ATA TGG CGA TCA GGC GAT G-3′ and 5′-ATC GG**A** TCC ATA GAG AGT TGC AGC TTG-3′. Restriction sites are underlined, the stop site is in italic, and base changes are in bold. The PCR-amplified untagged CueO fragment was inserted into expression plasmid pASK-IBA3 between the XbaI and PstI restriction sites.

All proteins were expressed in the absence of chloride ion, which was previously shown to bind CueO at the TNC (23). Accordingly, Tris-SO_4 buffer was used at all steps of purification in place of Tris-Cl. Proteins were loaded with the Cu(II) cofactor by addition of 5 mM $CuSO_4$ to the cell lysate, except for apo-CueO. Untagged CueO was purified using a new procedure. The protein was precipitated from the cell lysate by addition of $(NH_4)_2SO_4$ to 60% saturation followed by centrifugation (32,000 × *g*, 4 °C, 15 min) and redissolving the pellet in a minimal amount of 10 mM Tris-SO_4 buffer, pH 9.0. Excess salt was removed by extensive dialysis against 10 mM Tris-SO_4 buffer, pH 9.0, and the dialyzed protein was loaded onto a HighPrep

TABLE 1
X-ray data measurement and refinement statistics

Complex	Native	C500S Cu(II)	C500S Cu(I)	Ag(I)	ΔMet Cu(I)	Apo
Protein	Wild-type (untagged)	C500S (*Strep*-tag)	C500S (*Strep*-tag)	Wild-type (untagged)	Met-to-Ser (*Strep*-tag)	Copper-free (*Strep*-tag)
PDB code	3OD3	3NSC	3NT0	3NSD	3NSY	3NSF
Space group	$P2_1$	$P2_1$	$P2_1$	$P2_1$	$P2_1$	$P2_1$
Wavelength (Å)	0.9794	0.9002	0.9002	1.5418	1.3799	1.5418
Resolution (Å)[a]	1.1 (1.13–1.10)	1.5 (1.55–1.50)	1.8 (1.85–1.80)	2.0 (2.05–2.00)	2.1 (2.15–2.10)	2.0 (2.05–2.00)
Total reflections[a]	1,024,651/98,990	178,472/18,392	194,368/19,120	87,132/6911	103,795/10,237	117,974/11,595
Unique reflections[a]	188,928/18,866	72,799/6239	42,528/4,553	31,709/3,175	54,484/5499	30,192/3,018
Completeness (%)[a]	99/100	95/99	93.5/97	96/93	97.3/95.4	95/93
Mean I/σ_I[a]	8.4/2.5	10.1/1.9	8.4/2.1	7.5/2.1	11.2/4.7	12.6/2.9
R_{sym}[a,b]	0.084/0.354	0.056/0.244	0.150/0.330	0.080/0.334	0.043/0.131	0.097/0.353
Root mean square deviation bonds (Å)/angles (°)	0.011/1.5	0.018/1.8	0.014/1.5	0.016/1.7	0.012/1.4	0.011/1.3
R_{cryst}/R_{free}[a,c]	0.16/0.19	0.18/0.21	0.21/0.26	0.19/0.24	0.17/0.23	0.19/0.24
Mean B (Å^2)	16	27	17	34	33	31
Ramachandran plot: % favored (allowed)	96 (99)	98 (100)	97 (100)	97 (100)	96 (100)	97 (100)

[a] Overall/outermost shell.
[b] $R_{sym} = (\Sigma_h|I_h - \langle I\rangle|)/(\Sigma_h I_h)$, where $\langle I\rangle$ is the mean intensity of all symmetry-related reflections I_h.
[c] $R_{cryst} = (\Sigma||F_{obs}| - |F_{calc}||)/\Sigma|F_{obs}|$. R_{free} as for R_{cryst}, using a random subset of the data (5%) not included in the refinement. Reflections with $F > 0\ \sigma F$ were used in the refinement.

16/10 Sepharose Fast Flow (Amersham Biosciences) ion exchange column equilibrated with 10 mM Tris-SO_4 buffer at pH 9.0. Unbound protein was removed by washing with buffer (10 mM Tris-SO_4, pH 9.0) and bound protein was eluted with a linear gradient of 0–500 mM Na_2SO_4 in 10 mM Tris-SO_4 buffer, pH 9.0. Eluted fractions with $A_{610} > 0.05$ (Varian Cary 300) were pooled, concentrated, and loaded on to a Sephacryl size exclusion column to remove remaining contaminants. Eluted fractions displaying a 610-nm absorption band were pooled. The final material displayed a single band on an SDS-polyacrylamide gel upon staining with Coomassie dye and was estimated to be greater than 95% pure. UV-visible spectra of purified protein showed a ratio of $A_{280}/A_{610} = 11.0$, identical to that of CueO with intact *Strep*-tag. Apo-CueO was isolated and purified in the absence of added copper, resulting in a colorless, copper-free protein. Protein concentrations were determined spectroscopically (Varian Cary 300) using an ϵ_{280} of 63,036 M^{-1} cm^{-1}, which was estimated based on the protein sequence.

Steady-state Oxygen Consumption Kinetics—Steady-state Cu(I) and Fe(II) oxidase activities were measured as rates of oxygen consumption using an oxygraph (Hansatech, Cambridge, UK) as previously described (20). Stock solutions of the substrates were prepared in an anaerobic chamber. The substrate, Cu(I), was added as a complex, $[Cu(I)(MeCN)_4]PF_6$ (Sigma), and Fe(II) was added as the complex $Fe(NH_4)_2(SO_4)_2{\cdot}6H_2O$. Fe(II) oxidase activity was seen only in the presence of 1 mM Cu(II) added to the reaction mixture as $CuSO_4$. Steady-state Ag(I) inhibition kinetic measurements were made similarly to the Cu(I) oxidase activity measurements, except that the Cu(I) substrate concentration was held constant at 500 μM and the concentration of $AgNO_3$ was varied. Small (25 μl) aliquots of $AgNO_3$ (10 nM to 1 mM) were added into the reaction mixture (950 μl) containing 10 μg/ml of protein in 100 mM Tris acetate buffer, pH 5.0. A 25-μl aliquot of Cu(I) substrate, stored as a 20 mM stock solution of $[Cu(I)(MeCN)_4]PF_6$, was added to initiate the reaction. All kinetic measurements were made at 23 °C and pH 5.0. Activity measurements were plotted as a function of substrate or inhibitor concentration using SigmaPlot 7.0 (SSI, Richmond, CA) and kinetic constants, K_m and k_{cat}, were evaluated using a least-squares fit of a Michaelis-Menten curve. Enzyme velocities were plotted after subtracting the background contribution of enzyme-independent Cu(I) or Fe(II) oxidation.

Crystallization—Protein crystals were obtained by the hanging drop method as previously described (23). All CueO constructs were crystallized under identical conditions. For data measurement, crystals grown in 16% polyethylene glycol 4000, 0.2 M ammonium acetate, 0.1 M sodium acetate, pH 4.6, were transferred to an identical solution with a higher concentration of polyethylene glycol (30%). Metal-protein complexes were generated as follows: 1) C500S CueO + Cu(II), C500S CueO crystals were soaked in 25 mM $CuSO_4$ for 50 min; 2) C500S CueO + Cu(I), crystals of step 1 were reduced with 30 mM $Na_2S_2O_4$ (sodium dithionite) for 5 min before freezing; 3) ΔMet CueO + Cu(I), ΔMet CueO was treated with ~10 mM of the Cu(I) donating complex $[Cu(I)(MeCN)_4]PF_6$ for 2 min, resulting in a colorless crystal; 4) untagged CueO + Ag(I), untagged CueO was crystallized with 3 mM $AgNO_3$ included in the crystallization buffer.

X-ray Data Collection and Structure Determination—Crystals were picked up in a small loop (Hampton), cryo-cooled in liquid nitrogen, and diffraction data were measured at 100 K. Data for ΔMet CueO + Cu(I) and untagged CueO were collected at SSRL beamline 9-2 on a MAR325 detector. C500S CueO + Cu(II) and C500S CueO + Cu(I) data were collected at APS, beamline 14BM-C (BioCARS) on a Q315 detector. Diffraction data for apo-CueO and untagged CueO + Ag(I) were measured at 100 K on a Rigaku RUH3-R/R-Axis IV^{++} imaging plate system. All crystals were monoclinic, space group $P2_1$, with one molecule per asymmetric unit and cell parameters a = 50–51 Å, b = 91–92 Å, c = 54 Å, β = 103°. All data were processed with CrystalClear (29); data reduction statistics are given in Table 1. The structure of a tagged wild-type CueO (PDB codes 1KV7 (23) or 1N68 (24)) was used as a starting model for each of the new structures. Models were rebuilt with COOT (30), refined with REFMAC5 (31), and figures were prepared using PyMOL. The 1.1-Å structure was refined using anisotropic temperature factors; all others were refined isotropically. Other calculations were performed using the CCP4 package (32).

RESULTS

Complete Structure of CueO at 1.1-Å Resolution—Previous structures of CueO have only a portion of the methionine-rich insert (residues 355–400) sufficiently well ordered to be seen in the crystal (23–25). We produced a recombinant CueO without the C-terminal *Strep*-tag that was used in our previous studies in the hopes of finding a crystal form with the missing residues resolved and to ensure that the purification tag was not affecting activity. Spectra and catalytic activity for the highly pure untagged protein were indistinguishable from that of the tagged version and readily crystallized in the same crystal form as for the tagged protein. One such crystal yielded diffraction to 1.1-Å resolution, allowing for the interpretation of the missing residues.

The N-terminal portion of the methionine-rich insert (residues 355–379) contains Met^{355} and Asp^{360}, which are part of the sCu-binding site, a helical region that blocks access to the T1 and sCu sites (residues 356–371), and eight additional well ordered residues (372–379), as previously described (23, 24). The remainder of the insert (residues 380–399) and residues 400–402 were previously unseen but are now shown to form a loosely constrained loop lying across the methionine-rich helix and having few contacts with the rest of the protein (Fig. 1). Electron density, including side chains, was clear for residues 379–384 and 391–402, and somewhat discontinuous, but present for residues 385–390 (supplemental Fig. S1). The loop winds through a solvent-occupied region between CueO molecules in the crystal. In solution, this region is likely to be intrinsically disordered and only crystal packing constraints allow for the present conformation to be seen, even at 1.1-Å resolution. This 22-residue region contains 5 methionine and 5 histidine residues, and may provide additional Cu(I)- or Ag(I)-binding sites in solution when metal concentrations are high.

The remainder of the structure was very well defined. The C terminus was ordered and formed specific hydrogen bonds with the nitrogen atom of Ala^{490} and several water molecules; this region was essentially unchanged from that seen with the *Strep*-tag present. The T2 copper atom was slightly depleted in the structure and built as 75% occupied. An unknown ligand, possibly ethanediol, a PEG byproduct, was found bound to T2 and modeled in two orientations. A single oxygen atom was attached to one of the T3 copper atoms, consistent with the 1-electron reduced resting oxidized state and possibly resulting from hydrated electrons generated in the intense synchrotron x-ray beam. This same mixed oxidation state species has been seen in several laccase structures (PDB entries 1V10 (33), 1HFU (34), and 1A65 (35)). The trinuclear center geometry will be discussed in detail elsewhere.

Crystal Structures of C500S CueO + Cu(I) or Cu(II)—Cysteine 500 is one of the ligands of the T1 (*blue*) copper in CueO (Fig. 1). The C500S mutation results in a colorless protein that presumably lacks the T1 copper and has no catalytic activity (20). The UV-visible solution spectrum of C500S showed a complete loss of absorbance at 610 nm, consistent with the loss of blue color and catalytic activity (supplemental Fig. S2). MCO proteins with mutations that lead to loss of the T1 copper are often referred to as "T1D" for T1 copper depletion. To examine the role of the T1 copper in the loading of substrate copper at the sCu site and along the rest of the methionine-rich insert, we determined the crystal structures of the C500S mutant protein in the presence of either Cu(II) or Cu(I), the likely true CueO substrate.

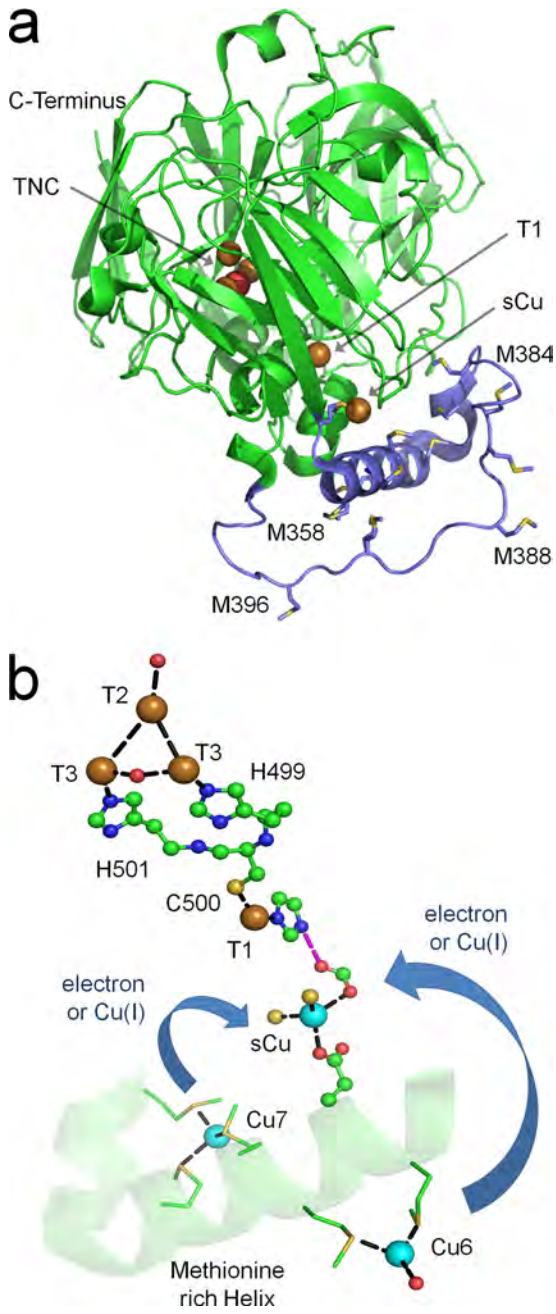

FIGURE 1. **CueO structure.** *a*, a ribbon diagram based upon PDB code 3OD3 (this work) showing the location of the TNC, T1, and sCu copper atoms (*bronze*), the TNC bridging oxygen atom (*red*), and the complete methionine-rich insert (*blue*). Side chains of methionine residues in the inset are shown; some have alternate conformations (not shown). The sCu site is not occupied in this structure but was added to the figure for reference. *b*, the electron transfer path in CueO. Cu(I) ions (*cyan*) are bound along the methionine-rich helix and at the sCu site. Electrons most likely proceed from sCu into the T1 site via a hydrogen bond (*pink dashed line*) between Asp^{439}, a sCu ligand, and His^{443}, a T1 ligand, and from there into the TNC and dioxygen (24). How Cu(I) is replenished at the sCu site is not yet known but may involve either direct transfer from the Cu6 and Cu7 sites, or through electron transfer (indicated by *blue arrows*). The view in *panel b* is rotated ~180° about the vertical axis with respect to *panel a*.

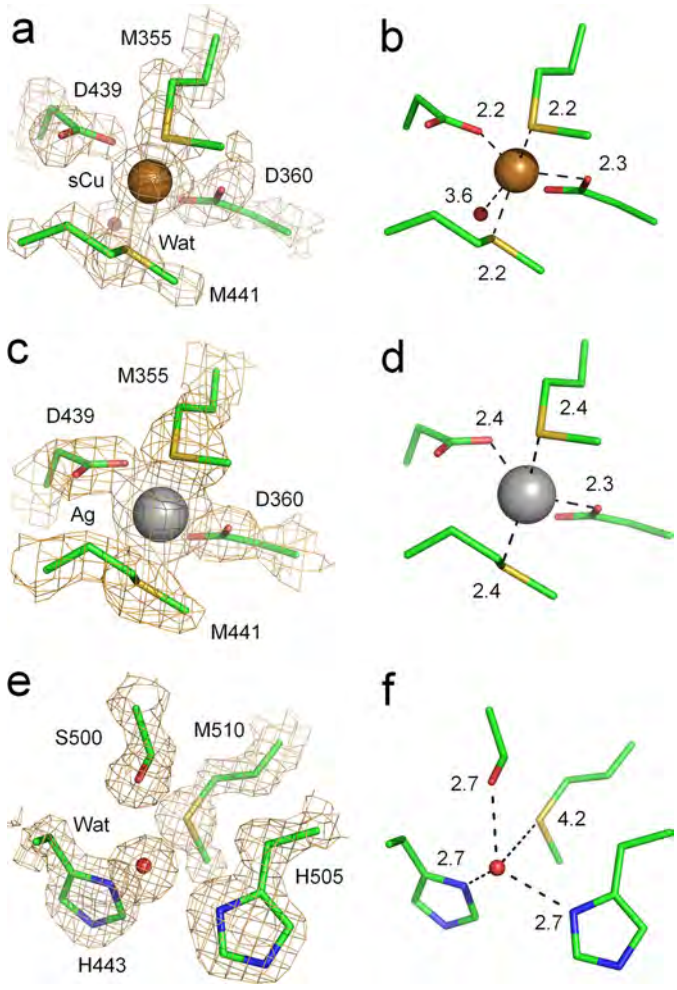

FIGURE 2. **Binding of metal at the sCu site and its absence at the T1 site in C500S CueO.** *a*, the sCu site is fully occupied with Cu(I) in C500S CueO + Cu(I). *b*, geometry of Cu(I) ligation. The water molecule shown was previously found to be coordinated with Cu(II), but is too far from Cu(I) in the present structure for coordination (3.6 Å). *c*, the sCu site is fully occupied with Ag(I) in CueO + Ag(I). *d*, geometry of Ag(I) ligation. *e*, the T1 site is occupied by a water molecule in C500S CueO. *f*, water molecule hydrogen bonding geometry. Electron density maps have been contoured at 1.5 σ. Distances are in Å.

C500S CueO crystallized under the same conditions as the wild-type protein. The Cu(II) complex was obtained by soaking C500S crystals in 25 mM $CuSO_4$ for 50 min followed by cryo-cooling. The Cu(I) complex was obtained by reducing the Cu(II) complex for 5 min with sodium dithionite, followed by cryo-cooling. Structures were determined at 1.5- and 1.8-Å resolution for the Cu(II) and Cu(I) complexes, respectively, and both are very similar to the wild-type protein, except at the copper-binding sites.

The C500S Cu(I) complex contained a copper atom at the sCu site much as previously described for the wild-type protein (24), consistent with Cu(I) binding as substrate (Fig. 2). However, unexpectedly, the sCu site was unoccupied on addition of Cu(II). We previously identified the sCu site through the soaking of Cu(II) into crystals of the wild-type protein (24). That it no longer binds to C500S suggests that binding of Cu(II) at the sCu site requires a functional T1 site. The reason for this is not yet clear.

Ser^{500} was well resolved in the Cu(II)-soaked crystal and the T1 site completely empty of copper, as expected (Fig. 2, *e* and *f*).

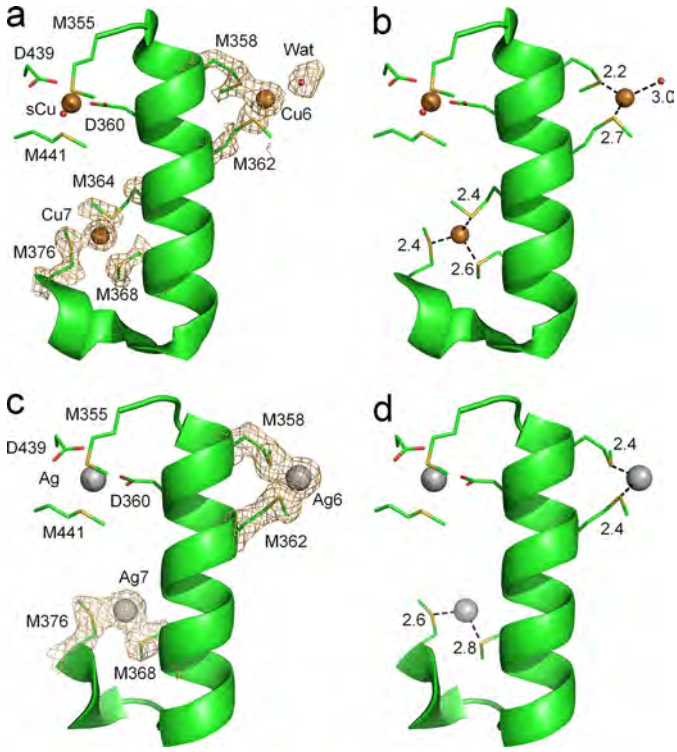

FIGURE 3. **Cu(I) and Ag(I) binding along the methionine-rich helix.** *a*, Cu(I) binding to C500S CueO, highlighting the Cu6 and Cu7 sites. Electron density for an unknown molecule has been modeled as water in the Cu6 site, but is more likely a histidine or methionine (see text). *b*, ligation geometry for Cu6 and Cu7. *c*, Ag(I) inhibitor ions bind CueO at the same sites as Cu(I) substrate ions in C500S CueO. *d*, ligation geometry for Ag6 and Ag7. Electron density maps have been contoured at 1.0 σ. Distances are in Å.

The T1 site was largely unchanged except for a slight expansion and the appearance of a well ordered water molecule that was ~0.9 Å from the position for the T1 copper in the wild-type protein and hydrogen bonded to Ser^{500}, His^{505}, and His^{443}. These three residues along with Met^{510} coordinate the T1 copper in the wild-type protein. The trinuclear copper centers in the Cu(I) and Cu(II) structures were much like that described above for the untagged protein, except that they both appeared to be incompletely photoreduced.

Binding of Cu(I) and Ag(I) to the Methionine-rich Insert—We and others have speculated that the methionine-rich insert might be used for copper binding as part of the response to copper toxicity (Fig. 1). The C500S Cu(I) structure, but not the Cu(II) structure, displayed two additional copper atoms bound to the methionine-rich helix (Fig. 3), supporting this hypothesis. Importantly, binding was limited to Cu(I), the more toxic of the copper ions and the probable CueO substrate.

Two Cu(I) ions, Cu6 and Cu7, were bound along the methionine-rich helix that blocks access to the sCu and T1 sites. A third, very low-occupancy copper site is near Met^{361} (Cu8, omitted in Fig. 3). Cu6 was coordinated through Met^{358} and Met^{362} and another ligand was presently modeled as a water molecule. The methionine ligands lay on the same face of the helix and were perfectly arranged to bind copper. Although we have placed a water molecule in the third ligand site for Cu6, the electron density for it is distinctly too large (Fig. 3). This, combined with the fact that water is an unlikely Cu(I) ligand, suggests that the third ligand was a methionine or a histidine side

chain from the disordered region (residues 380–403). Cu7 was coordinated through Met^{368} and Met^{376}, and a third, partially disordered residue, Met^{364} (Fig. 3).

There was no evidence of copper coordination at copper sites Cu6–8 in the Cu(II) structure. However, two additional copper ions, one bound to His^{488} on the protein surface and another bound to Met^{417} and His^{145}, were seen in both the Cu(I) and Cu(II) structures. These sites lie far from both the T1 and sCu sites and seem unlikely to be of functional importance.

To further explore the role of Cu(I) binding, and to ensure that the oxidation states for the copper atoms were correctly assigned, we turned to Ag(I), which has similar binding properties as Cu(I) but is relatively redox inert. The structure of untagged CueO co-crystallized with 3 mM Ag(I) revealed Ag(I) binding to the sCu site (*Ag* in Fig. 2) and to both major Cu(I)-binding sites along the methionine-rich helix (*Ag6* and *Ag7*, Fig. 3). All three sites expanded to accommodate the larger Ag(I) ion (~0.5 Å for the sCu site) and the coordination numbers decreased. The sCu site was fully occupied by silver, whereas Ag6 and Ag7 were only ~50% occupied, unlike Cu6 and Cu7, which were both fully occupied in the Cu(I) structure. Interestingly, Ag(I) did not displace copper at either the T1 or TNC sites. The Ag(I) crystals were blue, indicating that Cu(II) and not Ag(I) occupied the T1 site, and the ligation distances and electron densities at both the T1 and TNC sites were consistent with copper, not silver ligation. Taken together, the Cu(I), Cu(II), and Ag(I) results confirm that the methionine-rich region is able to bind additional Cu(I) ions.

Ag(I) Inhibition of CueO—To investigate whether Ag(I) could inhibit Cu(I) oxidase or Cu(II) stimulated Fe(II) oxidase activity in CueO, steady-state oxygen consumption rates were measured for untagged CueO at a saturating substrate concentration (500 μM Cu(I) or 500 μM Fe(II) + 1 mM Cu(II)) in the presence of increasing amounts of $AgNO_3$. Ag(I) sharply inhibited CueO: activity fell to 50% at ~1 μM Ag(I) and was essentially eliminated at 10 μM Ag(I) (Fig. 4*a*). No change in absorbance at 330 or 610 nm was seen until the Ag(I) concentration reached 1 mM (Fig. 4*b*), indicating inhibition was not due to displacement of the T1 or TNC copper atoms, consistent with the Ag(I) co-crystallization results described above, which also indicate that Ag(I) does not displace the T1 or TNC copper atoms. Taken together, these data indicate strong binding of Ag(I) at the sCu site abolishes CueO activity.

Copper Tolerance Assay: Inhibitory Effect of Ag(I) on Bacterial Copper Tolerance—Because Ag(I) binding at the sCu site makes CueO catalytically inactive, Ag(I) should also make bacteria dependent on the *cus* detoxification system for survival in the presence of environmental copper. To examine this, we measured cell growth for wild-type and *cus*-deleted *E. coli* strain W3110 in the presence and absence of Ag(I) (Fig. 5). When Ag(I) was absent, there was no difference in the growth of wild-type and *cus*-deleted strains, consistent with previous findings (1). However, addition of just 5 μM Ag(I) to the growth media led to marked copper sensitivity in the *cus*-deleted strain, whereas the wild-type strain survived copper stress nearly as well as in the absence of Ag(I). These results suggest that the *cus* system plays a specific role in aerobic copper tolerance by overcoming Ag(I) poisoning of the *cue* system.

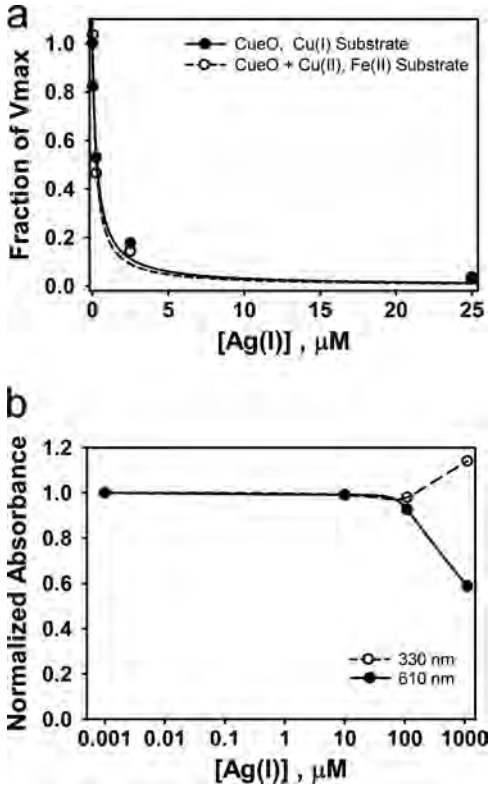

FIGURE 4. **Ag(I) inhibition of CueO activity.** *a*, steady-state kinetic measurements of oxygen consumption by untagged CueO (0.2 μM, pH 5.0, 23 °C) with either Cu(I) (*closed circles*) or Fe(II) (*open circles*) as substrate, in the presence of increasing amounts of Ag(I) inhibitor. Plotted is the fraction of maximum activity ([Ag(I)] = 0) as a function of Ag(I) concentration at constant saturating concentration of substrate (500 μM Cu(I) or 500 μM Fe(II) + 1 mM Cu(II)). The *solid* and *dashed lines* are inverse hyperbolic fits to the *closed circles* (Cu(I) oxidation) and *open circles* (Fe(II) oxidation), respectively. *b*, fractional changes in the absorbance at 330 (*open circles*) and 610 nm (*closed circles*) upon titration of 30 μM untagged CueO with Ag(I). Plotted is absorbance at each Ag(I) concentration normalized with respect to the absorbance at [Ag(I)] = 0. No loss of absorbance at 330 or 610 nm was observed until the Ag(I) concentration exceeded 100 μM (3.3-fold excess Ag(I)), well above the level at which complete inhibition occurs. Co-crystallization of 1 mM CueO with 3 mM Ag(I) led to a structure with the T1 copper fully occupied (see text).

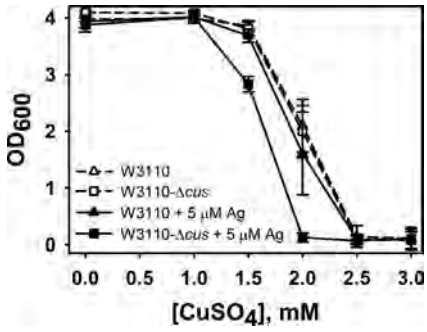

FIGURE 5. **Protective effect of the *cus* system on Ag(I) inhibition of copper tolerance in *E. coli*.** Plotted is cell growth for wild-type *E. coli* strain W3110 (*triangles*) and mutant *E. coli* W3110-Δ*cus* strain *GR6* (*squares*) as a function of [$CuSO_4$] in the absence (*open symbols*) or presence of 5 μM Ag(I) (*closed symbols*). Plotted is the mean ± S.D. of three measurements for each condition. Cell growth was measured as the optical cell density at 600 nm (A_{600}).

Crystal Structure of ΔMet CueO + Cu(I): Necessity of Methionine Residues for Cu(I) Binding—All six methionine residues along the methionine-rich helix (Met^{358}, Met^{361}, Met^{362}, Met^{364}, Met^{366}, and Met^{368}), including four of the five methionine residues shown above to bind Cu(I) and Ag(I), were

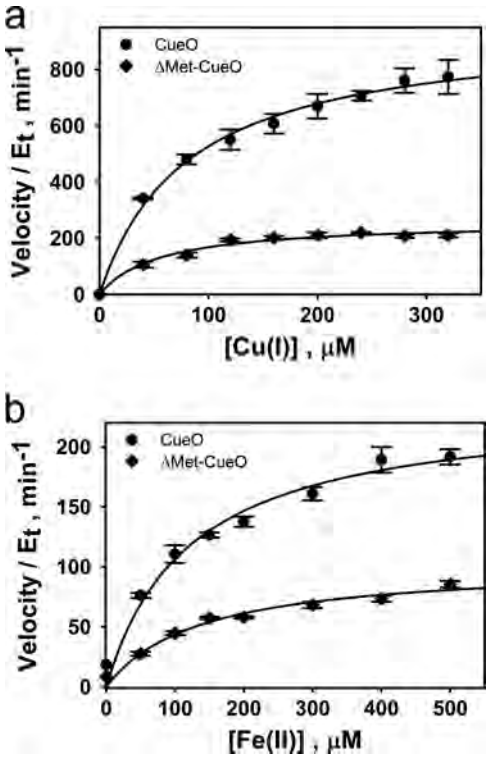

FIGURE 6. **Steady-state kinetic measurements of oxygen consumption rates by wild-type and ΔMet CueO.** *a,* Cu(I) as substrate. *b,* Fe(II) as substrate. Plotted are the mean ± S.D. of the initial oxygen consumption rate ($n = 3$) by wild-type CueO (*circles*) and ΔMet CueO (*diamonds*) upon addition of substrate at varying concentrations. The *solid lines* are a nonlinear fit of the Michaelis-Menten equation through the plotted data, yielding K_m and k_{cat} values (see Table 2).

mutated to serine to disrupt Cu(I) binding at these locations. The crystal structure of this mutant protein in the presence of Cu(I), and containing a reduced T1 copper site, was determined at 2.1-Å resolution, revealing a protein with an overall structure essentially identical to that of the wild-type protein (Cα root mean square deviation = 0.3 Å). The helical fold at the site of the mutations remained intact; however, Cu(I) binding along the helix was completely abolished (supplemental Fig. S3), whereas Cu(I) occupancy at the sCu site was reduced to ~50%. No notable differences in copper binding were found at the TNC, except for a greater depletion of the T2 copper, the most labile of the three, which was only ~50% occupied.

ΔMet CueO Kinetics and Spectra—We investigated Cu(I) oxidase activity in ΔMet CueO to evaluate the role of the methionine-rich helix in catalysis. The steady-state Cu(I) and Fe(II) oxidase activities of the wild-type and ΔMet proteins were measured in terms of rates of oxygen consumption (Fig. 6), and the resulting K_m and k_{cat} values were tabulated as shown in Table 2. Although K_m was largely unchanged between the wild-type and ΔMet proteins, k_{cat} for Cu(I) oxidase activity decreased 4-fold, and Fe(II) oxidase activity 2-fold, in the ΔMet mutant. It is important to note that the measured K_m in these experiments should be viewed as an upper limit, because it does not directly measure the free concentration of Cu(I), which is highly labile, but rather the concentration of Cu(I) released from the acetonitrile delivery complex (20). Kinetic parameters for untagged and *Strep*-tagged CueO proteins were essentially identical (data not shown).

TABLE 2
Kinetic parameters for CueO proteins

Parameters were determined from steady-state oxygen consumption rates using 280 nM protein at pH 5.0 and 23 °C. Protein concentrations were determined from absorption at 280 nm. For Fe(II) oxidation, 1 mM $CuSO_4$ was included in the reaction mixture and Fe(II) added as $Fe(NH_4)_2(SO_4)_2 \cdot 6H_2O$. For Cu(I) oxidation, the Cu(I) donating complex $[Cu(I)(MeCN)_4]PF_6$ was used.

	Fe(II) oxidation		Cu(I) oxidation
	CueO	ΔMet CueO	CueO
k_{cat} (min^{-1})	235 ± 16	102 ± 8	952 ± 30
K_m (μM)	120 ± 25	135 ± 31	81 ± 8

The spectrum of ΔMet CueO as isolated showed a roughly 2-fold higher ratio of A_{280}/A_{333} and A_{280}/A_{613} as compared with wild-type CueO, suggesting depletion or reduction of copper centers in this mutant (supplemental Fig. S4). However, the ΔMet CueO + Cu(I) structure showed that although the T2 and sCu coppers were partially depleted, the T1 copper, which is responsible for the A_{613} band, was fully occupied. Because the protein was isolated in the presence of excess copper, and all kinetic measurements were performed with excess copper, the weaker A_{613} and A_{333} bands in the mutant protein spectra may be due to partial T1 reduction caused by partial depletion of T2.

Crystal Structure of Apo-CueO—Many MCO crystal structures display partial depletion of the four catalytic copper ions. In particular, the T2 copper is easily lost (25, 35–37) and a crystal structure of CueO with T2 removed, and T1 and T3 partially depleted, has been described (erroneously referred to as apo-CueO (25)). Apo-CueO prepared in the absence of added copper to cells can be reconstituted by titration with Cu(II) in the form of copper sulfate (38); reconstitution of other MCOs can also be achieved, but apparently only with Cu(I) (39). Thus, despite the structurally critical locations of the catalytic copper atoms, it appears that most MCOs either fold properly in the absence of copper or remain properly folded when copper is chemically extracted. The exception is ceruloplasmin, for which the loss of the T3 copper atoms, located at the interface between domains 1 and 3, leads to partial unfolding (40).

We determined the structure of apo-CueO to further explore this issue (2.0-Å resolution, Table 1). The protein was prepared without addition of copper to the cell lysate during purification, leading to a colorless purified protein. The resulting structure is essentially identical to that for the holoprotein (PDB entry 1KV7 (23), Cα root mean square deviation = 0.16 Å), except for the complete absence of copper at any of the copper sites. A single water molecule occupies the TNC and is located at a position halfway between the two T3 copper positions in the native protein at distances ranging from 2.7 to 3.8 Å from the eight histidine residues normally coordinating copper. The T1 and sCu copper sites are empty, with no evidence of bound water. Cys^{500}, Met^{510}, and His^{443} and His^{505}, which normally coordinate the T1 copper, are unchanged in position in comparison with the wild-type protein (PDB entries 1KV7 (23) and 1N68 (24)). The 24-residue region generally disordered in CueO structures (residues 379–403) was somewhat better ordered in the apocrystal, allowing for residues 395–402 to be added to the model.

CueO is transported to the periplasm using the twin-arginine protein translocase, which transports fully folded proteins (41).

Because CueO readily folds into its native state in the absence of copper and will apparently take up either Cu(I) or Cu(II), both of which are kept in low concentrations in the cytosol, it may be that CueO is secreted into the periplasm in its folded but copper-free apo form and becomes catalytically competent there only as copper ions appear. However, because CueO is only expressed when copper ions are present, loading may take place before transport. That each copper-binding site is preformed in the apoprotein, and without well ordered water molecules that might compete with copper loading, suggests activation in either compartment is likely to be a rapid process.

DISCUSSION

Although methionine-rich sequences are common in bacterial copper detoxification systems, molecular details of both structure and function are lacking. Here, we present the 1.1-Å crystal structure of CueO with its entire methionine-rich region revealed (Fig. 1). We also present crystal structures of the Cu(I) CueO complex, which confirms Cu(I) binding to the sCu site and reveals Cu(I) binding to two new sites, Cu6 and Cu7. In each of these Cu(I)-binding sites, the metal ion is ligated by methionine residues from the methionine-rich region (Figs. 2 and 3). Removal of the Cu6 and Cu7 sites through mutation leads to a protein with 4-fold reduced catalytic rates for oxidation of Cu(I) (Table 2), while retaining its native fold (supplemental Fig. S3). Ag(I) binds to all three Cu(I)-binding sites, inhibiting CueO at low micromolar concentrations *in vitro* and disabling the *cue* system *in vivo*, necessitating the use of the *cus* system for copper tolerance in *E. coli* exposed to silver.

The MCOs found in many bacterial copper detoxification systems (28, 42, 43) have both methionine-rich sequences and cuprous oxidase activity. We have shown that Cu(I) binds to at least two sites along the CueO methionine-rich sequence near the sCu site, and these binding sites are specific for the cuprous ion; no metal binding was found at the sCu, Cu6, and Cu7 sites in crystals of C500S CueO soaked with Cu(II). In the wild-type protein, loading of the sCu site with Cu(II) does occur (24), but this is apparently a redox-dependent event and requires a functional T1 site. We showed previously that removal of the sCu site leads to a dramatically impaired enzyme (24). This, taken together with reduced CueO activity when the methionine residues comprising the Cu6- and Cu7-binding sites are mutated to serine, strengthens the argument that the methionine-rich insert facilitates Cu(I) oxidation. The mechanism for this is not yet clear, but is likely to involve either direct transfer of Cu(I) from the Cu6 and Cu7 sites into the sCu site, or provision of a path for electron transfer from Cu6 and Cu7 to sCu, and from there to the catalytic copper atoms (Fig. 1). The methionine-rich insert provides for substrate discrimination because it buries the T1 site; its deletion results in a protein with decreased Cu(I) oxidase activity and an increased ability to oxidize organic substrates in the absence of added copper, presumably through increased access to the T1 site (44).

A recent detailed kinetic analysis of Cu(I) oxidation by CueO, where Cu(I) was provided as a $[Cu(Bca)_2]^{3-}$ complex, concluded that Cu(I) must be bound to the sCu site to be oxidized and the authors argued for a direct transfer of Cu(I) from the complex to the sCu site (21). They also report a subpicomolar dissociation constant for Cu(I) to the sCu site, a value similar to that for the $(Bca)_2$ complex itself. Because the sCu site is not solvent exposed, it is more likely that direct transfer occurs to substrate-binding sites in the methionine-rich region and from there to the sCu site (Fig. 1). Although we have identified two Cu(I)-binding sites in this region, the 24 residues unseen in the Cu(I)-soaked C500S CueO structure may provide additional Cu(I)-binding sites.

Cu(I) is bound along the methionine-rich region using thioether ligation. Cu7 displays a clear Met_3-Cu(I) configuration, whereas Cu6 displays a Met_2X-Cu(I) configuration with the third ligand (X) uninterpretable in the electron density map and modeled as water (Fig. 3). This third ligand is most likely Met^{393}, His^{395}, Met^{396}, or His^{398} from the disordered portion of the methionine-rich region, based on the location of these residues in the unliganded high resolution structure. Although uncommon, structures of proteins with Met_2-Cu(I) or Met_3-Cu(I) are known, including Met_2His-Cu(I) binding in PcoC (45) and Met_2His-Cu(I) binding in CusF (9). The latter is further stabilized by a unique cation-π interaction between the metal ion and a tryptophan ring (14, 46). The low coordination number, solvent exposure, and disorder of the methionine-rich binding sites in CueO make them suitable for transient copper binding and substrate procurement.

Ag(I) is a potent inhibitor of CueO oxidase activity: as little as 5 μM Ag(I) in the growth media suppresses copper resistance in *E. coli* (Fig. 5) and nearly eliminates Cu(I) oxidase activity for CueO *in vitro* (Fig. 4). Ag(I) binds to CueO at all three identified Cu(I) sites (Fig. 3), blocking Cu(I) substrate binding and preventing electron transfer from Cu(I) to the T1 copper atom. This provides a simple, clear explanation for silver inhibition of CueO activity.

Copper detoxification systems must function in the presence of silver because these metals often occur together in nature and their similar ligand-binding chemistries make them competitors (11–13). The *cue* and *cus* systems of *E. coli*, and copper detoxification systems in general, bind and transport both Ag(I) and Cu(I). CopA, the second component of the *E. coli cue* system, is induced by Ag(I) and transports Ag(I) across the cytoplasmic membrane almost as efficiently as Cu(I). However, for *E. coli* to survive mixed copper/silver stress, Ag(I) must be removed not only from the cytoplasm but also from the periplasm to prevent CueO inhibition. Inclusion of the *cus* system, which serves to export Ag(I) from the periplasm (11, 47), allows for full copper tolerance, whereas its removal greatly sensitizes *E. coli* to copper stress in the presence of even small Ag(I) quantities (Fig. 5). Thus, it appears that even in aerobic conditions the *cus* system is important for copper tolerance, becoming necessary when silver is present.

Acknowledgments—The SSRL Structural Molecular Biology Program is supported by the Department of Energy, Office of Biological and Environmental Research, and by the National Institutes of Health, National Center for Research Resources, Biomedical Technology Program, and the NIGMS. Diffraction data were also measured at BioCARS Sector 14, Advanced Photon Source, Argonne National Laboratory, supported by the United States Department of Energy under Contract W-31-109-Eng-38. BioCARS is supported by the National Institutes of Health, National Center for Research Resources Grant RR07707.

REFERENCES

1. Outten, F. W., Huffman, D. L., Hale, J. A., and O'Halloran, T. V. (2001) *J. Biol. Chem.* **276,** 30670–30677
2. Rensing, C., and Grass, G. (2003) *FEMS Microbiol. Rev.* **27,** 197–213
3. Grass, G., and Rensing, C. (2001) *J. Bacteriol.* **183,** 2145–2147
4. Grass, G., and Rensing, C. (2001) *Biochem. Biophys. Res. Commun.* **286,** 902–908
5. Rensing, C., Fan, B., Sharma, R., Mitra, B., and Rosen, B. P. (2000) *Proc. Natl. Acad. Sci. U.S.A.* **97,** 652–656
6. Changela, A., Chen, K., Xue, Y., Holschen, J., Outten, C. E., O'Halloran, T. V., and Mondragón, A. (2003) *Science* **301,** 1383–1387
7. Outten, F. W., Outten, C. E., Hale, J., and O'Halloran, T. V. (2000) *J. Biol. Chem.* **275,** 31024–31029
8. Franke, S., Grass, G., Rensing, C., and Nies, D. H. (2003) *J. Bacteriol.* **185,** 3804–3812
9. Loftin, I. R., Franke, S., Roberts, S. A., Weichsel, A., Héroux, A., Montfort, W. R., Rensing, C., and McEvoy, M. M. (2005) *Biochemistry* **44,** 10533–10540
10. Bagai, I., Rensing, C., Blackburn, N. J., and McEvoy, M. M. (2008) *Biochemistry* **47,** 11408–11414
11. Franke, S., Grass, G., and Nies, D. H. (2001) *Microbiology* **147,** 965–972
12. Stoyanov, J. V., Hobman, J. L., and Brown, N. L. (2001) *Mol. Microbiol.* **39,** 502–511
13. Stoyanov, J. V., Magnani, D., and Solioz, M. (2003) *FEBS Lett.* **546,** 391–394
14. Loftin, I. R., Franke, S., Blackburn, N. J., and McEvoy, M. M. (2007) *Protein Sci.* **16,** 2287–2293
15. Stout, J. E., and Yu, V. L. (2003) *Infect. Control Hosp. Epidemiol.* **24,** 563–568
16. Silver, S. (2003) *FEMS Microbiol. Rev.* **27,** 341–353
17. Cooksey, D. A. (1994) *FEMS Microbiol. Rev.* **14,** 381–386
18. Solomon, E. I., Augustine, A. J., and Yoon, J. (2008) *Dalton Trans.* 3921–3932
19. Solomon, E. I., Sundaram, U. M., and Machonkin, T. E. (1996) *Chem. Rev.* **96,** 2563–2606
20. Singh, S. K., Grass, G., Rensing, C., and Montfort, W. R. (2004) *J. Bacteriol.* **186,** 7815–7817
21. Djoko, K. Y., Chong, L. X., Wedd, A. G., and Xiao, Z. (2010) *J. Am. Chem. Soc.* **132,** 2005–2015
22. Kosman, D. J. (2010) *J. Biol. Inorg. Chem.* **15,** 15–28
23. Roberts, S. A., Weichsel, A., Grass, G., Thakali, K., Hazzard, J. T., Tollin, G., Rensing, C., and Montfort, W. R. (2002) *Proc. Natl. Acad. Sci. U.S.A.* **99,** 2766–2771
24. Roberts, S. A., Wildner, G. F., Grass, G., Weichsel, A., Ambrus, A., Rensing, C., and Montfort, W. R. (2003) *J. Biol. Chem.* **278,** 31958–31963
25. Li, X., Wei, Z., Zhang, M., Peng, X., Yu, G., Teng, M., and Gong, W. (2007) *Biochem. Biophys. Res. Commun.* **354,** 21–26
26. Puig, S., and Thiele, D. J. (2002) *Curr. Opin. Chem. Biol.* **6,** 171–180
27. Wernimont, A. K., Huffman, D. L., Finney, L. A., Demeler, B., O'Halloran, T. V., and Rosenzweig, A. C. (2003) *J. Biol. Inorg. Chem.* **8,** 185–194
28. Cha, J. S., and Cooksey, D. A. (1991) *Proc. Natl. Acad. Sci. U.S.A.* **88,** 8915–8919
29. Pflugrath, J. W. (1999) *Acta Crystallogr. D Biol. Crystallogr.* **55,** 1718–1725
30. Emsley, P., Lohkamp, B., Scott, W. G., and Cowtan, K. (2010) *Acta Crystallogr. D Biol. Crystallogr.* **66,** 486–501
31. Murshudov, G. N., Vagin, A. A., and Dodson, E. J. (1997) *Acta Crystallogr. D Biol. Crystallogr.* **53,** 240–255
32. (1994) *Acta Crystallogr. D Biol. Crystallogr.* **50,** 760–763
33. Garavaglia, S., Cambria, M. T., Miglio, M., Ragusa, S., Iacobazzi, V., Palmieri, F., D'Ambrosio, C., Scaloni, A., and Rizzi, M. (2004) *J. Mol. Biol.* **342,** 1519–1531
34. Ducros, V., Brzozowski, A. M., Wilson, K. S., Ostergaard, P., Schneider, P., Svendson, A., and Davies, G. J. (2001) *Acta Crystallogr. D Biol. Crystallogr.* **57,** 333–336
35. Ducros, V., Brzozowski, A. M., Wilson, K. S., Brown, S. H., Ostergaard, P., Schneider, P., Yaver, D. S., Pedersen, A. H., and Davies, G. J. (1998) *Nat. Struct. Biol.* **5,** 310–316
36. Hakulinen, N., Kiiskinen, L. L., Kruus, K., Saloheimo, M., Paananen, A., Koivula, A., and Rouvinen, J. (2002) *Nat. Struct. Biol.* **9,** 601–605
37. Piontek, K., Antorini, M., and Choinowski, T. (2002) *J. Biol. Chem.* **277,** 37663–37669
38. Galli, I., Musci, G., and Bonaccorsi di Patti, M. C. (2004) *J. Biol. Inorg. Chem.* **9,** 90–95
39. Musci, G., Di Marco, S., Bellenchi, G. C., and Calabrese, L. (1996) *J. Biol. Chem.* **271,** 1972–1978
40. Vachette, P., Dainese, E., Vasyliev, V. B., Di Muro, P., Beltramini, M., Svergun, D. I., De Filippis, V., and Salvato, B. (2002) *J. Biol. Chem.* **277,** 40823–40831
41. Palmer, T., Sargent, F., and Berks, B. C. (2005) *Trends Microbiol.* **13,** 175–180
42. Fernandes, A. S., Gaspar, J., Cabral, M. F., Caneiras, C., Guedes, R., Rueff, J., Castro, M., Costa, J., and Oliveira, N. G. (2007) *J. Inorg. Biochem.* **101,** 849–858
43. Lee, S. M., Grass, G., Rensing, C., Barrett, S. R., Yates, C. J., Stoyanov, J. V., and Brown, N. L. (2002) *Biochem. Biophys. Res. Commun.* **295,** 616–620
44. Kataoka, K., Komori, H., Ueki, Y., Konno, Y., Kamitaka, Y., Kurose, S., Tsujimura, S., Higuchi, Y., Kano, K., Seo, D., and Sakurai, T. (2007) *J. Mol. Biol.* **373,** 141–152
45. Peariso, K., Huffman, D. L., Penner-Hahn, J. E., and O'Halloran, T. V. (2003) *J. Am. Chem. Soc.* **125,** 342–343
46. Loftin, I. R., Blackburn, N. J., and McEvoy, M. M. (2009) *J. Biol. Inorg. Chem.* **14,** 905–912
47. Lok, C. N., Ho, C. M., Chen, R., Tam, P. K., Chiu, J. F., and Che, C. M. (2008) *J. Proteome Res.* **7,** 2351–2356

SUPPLEMENTAL MATERIAL

CRYSTAL STRUCTURES OF MULTICOPPER OXIDASE CUEO BOUND TO COPPER(I) AND SILVER(I): FUNCTIONAL ROLE OF A METHIONINE-RICH SEQUENCE*

Satish K. Singh, Sue A. Roberts, Sylvia Franke McDevitt, Andrzej Weichsel, Guenter F. Wildner, Gregor B. Grass, Christopher Rensing and William R. Montfort

Table of Contents

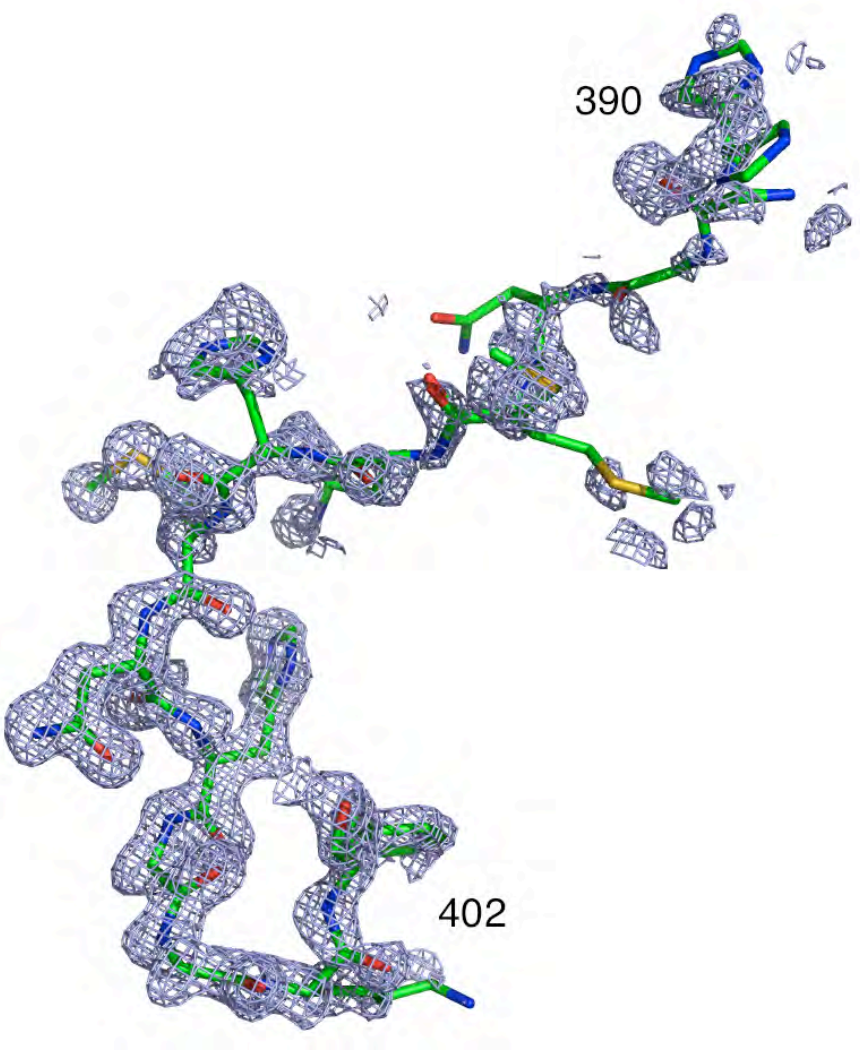

FIGURE S1. **Electron density for the omitted methionine-rich loop.** Representative electron density for the methionine-rich insert (residues 380 – 402) after omission from the model and refinement for 12 cycles to remove model bias. Shown is difference electron density for residues 390 – 402, contoured at 2.0 σ. The density is discontinuous for residues 383 – 392 in the map, but the general path for the chain can be discerned. Residues at either end of this stretch (380 – 382 and 393 – 402) are more reliably placed. Temperature factors for backbone atoms in the 380 – 402 stretch refined to values ranging between 24 and 82 $Å^2$.

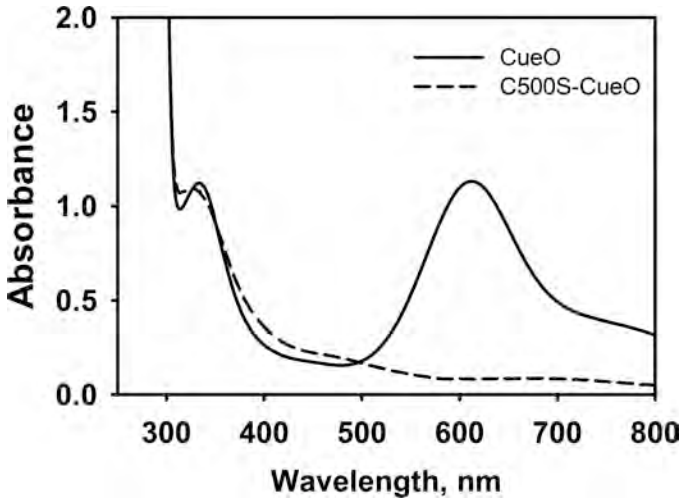

FIGURE S2. **UV-visible spectra of C500S CueO.** Absorption spectra of C500S (dashed line) and wild-type CueO (solid line) are shown. Note the lack of 610 nm absorbance peak in C500S and the presence of a broad absorbance peak at ~470 nm, which has previously been attributed to a peroxide-bound TNC.

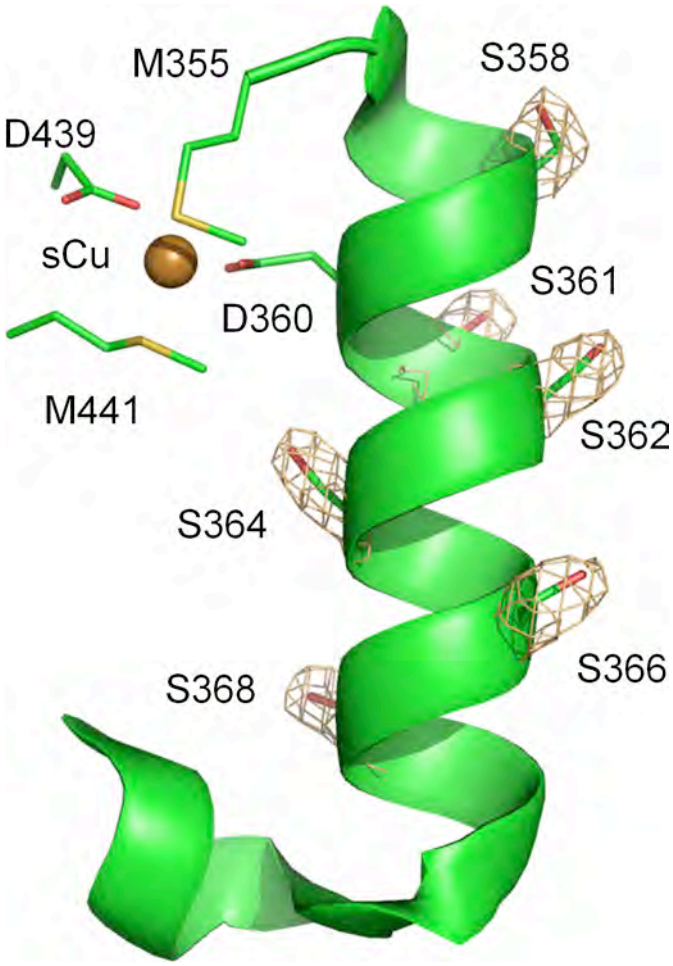

FIGURE S3. **Ribbon diagram of ΔMet CueO.** The helical structure containing the methionine-to-serine mutations is unchanged in the structure of ΔMet CueO + Cu(I) and the serine residues are well ordered. Copper binding at the sCu site is intact (density not shown), but is completely absent along the helix. Electron density has been contoured at 1.5 σ.

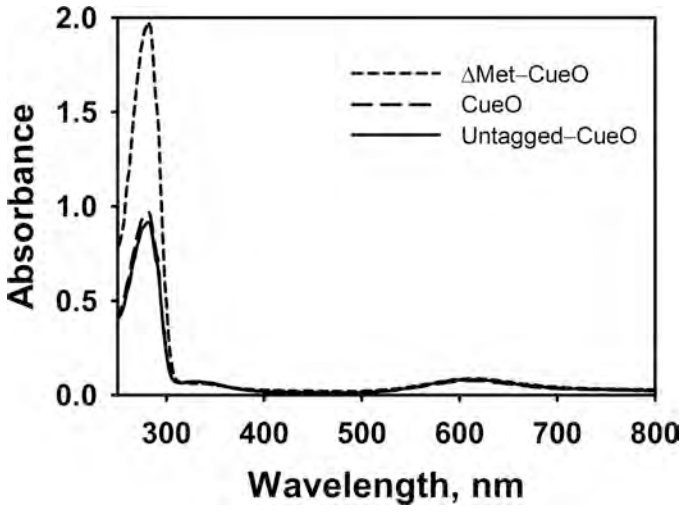

FIGURE S4. **UV-visible spectra of ΔMet CueO.** Absorption spectra of ΔMet CueO (short-dashed line), CueO (long-dashed line) and untagged CueO (solid line) are shown. Note the increased A_{280}:A_{610} ratio in ΔMet CueO, which may be due to partial T1 reduction (see main text).

Crystal Structures of Multicopper Oxidase CueO Bound to Copper(I) and Silver(I): FUNCTIONAL ROLE OF A METHIONINE-RICH SEQUENCE

Satish K. Singh, Sue A. Roberts, Sylvia F. McDevitt, Andrzej Weichsel, Guenter F. Wildner, Gregor B. Grass, Christopher Rensing and William R. Montfort

J. Biol. Chem. 2011, 286:37849-37857.
doi: 10.1074/jbc.M111.293589 originally published online September 8, 2011
